Integral (n,γ) Cross-sections Measurement of Standard Light Water Reactors Materials

A. Gruel, B. Geslot, A. Pepino, J Salvo, P. Leconte, P. Blaise

Integral (n,γ) Cross-sections Measurement of Standard Light Water Reactors Materials

A. Gruel[1], B. Geslot[1], A. Pepino[1], J. Di Salvo[1], P. Leconte[2], P. Blaise[1]

1) CEA, DEN, DER/SPEx, Cadarache, F-13108 St Paul lez Durance
2) CEA, DEN, DER/SPRC, Cadarache, F-13108 St Paul lez Durance

Corresponding author: adrien.gruel@cea.fr

Abstract. MAESTRO is an experimental program in support of the French nuclear industry recently carried out in the MINERVE facility. MINERVE is a pool type zero power reactor (ZPR), well known for being equipped with an oscillating device that makes it possible to measure small-sample reactivity with a very high precision (< 0.1 pcm). MAESTRO is devoted to the improvement of neutron cross sections of elements such as neutron absorbers, detection materials and reactor structure materials widely used in Gen-II and –III pressurized water reactors (PWRs). Neutron activation and pile-oscillation techniques are used together to provide complementary information on the capture and scattering cross sections through the measurement of isotopic capture rate and global reactivity-worth for each material. Samples of high elemental purity have been manufactured to reach a target accuracy of < 2 % (1 σ) on the measurement. This paper focuses on neutron activation measurements performed on several absorbing materials. The capture rates of 16 isotopes were studied by gamma spectrometry on their activation products: Eu-151, Eu-153, In-113, In-115, Ag-109, Cs-133, Mo-98, Mo-100, Sn-112, Sn-116, Sn-122, V-51, Zn-64, Zn-68, Zr-94 and Zr-96. Cadmium ratio measurements were also carried out on small dosimeters of gold, silver, cesium and indium. Since gold is generally considered as a reference element, results are constructed as ratios of the capture rates of interest to the gold capture rate. This procedure eliminates possible systematic errors and reduces uncertainties coming from the detector calibration. The complete uncertainty analysis is presented and discussed along with the experimental results.

1. Introduction

The MAESTRO experimental program is devoted to the improvement of radiative capture cross sections of elements such as neutron absorbers, detection materials and reactor structure materials widely used in Gen-II and –III pressurized water reactors (PWRs). The materials at stake are involved in several applications for light water reactors:

- reactivity of structural materials and industrial alloys;
- instrumentation for flux monitoring;
- reactivity control with innovative neutron absorbers;
- burn-up credit.

Previous programs were devoted to the improvement of fission products [1], neutron absorbers [2] or actinides [3] nuclear data, carried out in the MINERVE Zero Power Reactor (ZPR) [4].

This paper is focused on neutron activation measurements performed in the framework of the MAESTRO program held between 2013 and 2014. 9 pure elemental samples were irradiated, leading to the measurement of the radiative capture rate of 16 isotopes: ^{151}Eu, ^{153}Eu, ^{113}In, ^{115}In, ^{109}Ag, ^{133}Cs, ^{98}Mo, ^{100}Mo, ^{112}Sn, ^{116}Sn, ^{122}Sn, ^{51}V, ^{64}Zn, ^{68}Zn, ^{94}Zr and ^{96}Zr. The gold capture cross section being considered as a standard, 4 gold samples were used as references.

The first part of this paper describes the experimental setup: reactor configuration, description of the samples, the irradiation setup, the gamma spectrometry bench.

The second part describes the data processing and the associated results. Activation measurements results are presented as ratios of capture rates to the gold capture rate of 4 reference samples.

2. Experimental set up

2.1 Reactor configuration

MINERVE is a pool type reactor operated by CEA (Cadarache, France). Its core is divided into two zones. An outer driver zone is loaded with large reflector graphite blocks and highly enriched ^{235}U fuel plates. An inner experimental lattice zone, loaded in the 70x70 cm square cavity at the center of the driver zone. It is a 1.26 cm square pitch lattice of approximately 800 UO_2 fuel pins at 3 % enrichment in ^{235}U (FIG 1).

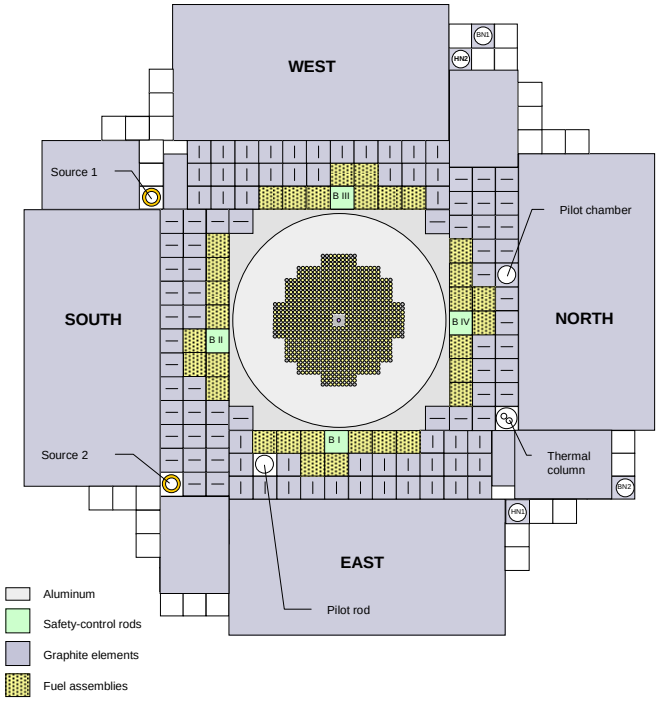

FIG 1: Schematic view of the MINERVE core.

Samples are put into an air-tight oscillating device. A solid aluminum block is placed at the center of the lattice. It is hollowed at its center to let past the oscillating device. A pilot rod with cadmium sectors placed inside a reflector block, outside the driver zone, is used to compensate for small reactivity variations.

During the design phase, effort has been made to reduce experimental uncertainties as low as possible. The water gap between the oscillating device and the aluminum block is 0.1 mm, ensuring a precise radial positioning of the sample in the core. The oscillating device is water-proof, meaning that there is only air around the sample or detector. This significantly decreases the final uncertainty contribution due to the clad diameter uncertainty.

The neutron spectrum at the irradiation position is very close to a standard PWR spectrum. At the center of the core inside the oscillation channel, about 15.5 % of the neutrons are in the thermal energy domain (below 0.63 eV), 39 % in the 0.63 eV to 100 keV range, and 45.5 % above 100 keV.

2.2 Samples and detectors characteristics

During the MAESTRO program, 9 samples and 4 reference gold samples were irradiated several times (up to 3 times). Their characteristics are given in Table I. Most of the samples are inserted in an aluminum clad of 10 x 12 mm in diameter and 110 (inside) x 120 (outside) mm long, with screwed-in end-plugs.

TABLE I: Samples characteristics.

Sample	Element	Mass of element	Type	Height	Diameter
M-Eu	^{nat}Eu	0.048 g	Solution	100 mm	8.35 mm
M-In-2	^{nat}In	0.275 g	Solution	100 mm	8.35 mm
M-Ag-2	^{nat}Ag	1.658 g	Solution	100 mm	8.35 mm
M-Cs-2	^{nat}Cs	0.917 g	Solution	100 mm	8.35 mm
M-Mo	^{nat}Mo	29.094 g	Rod	100 mm	6 mm
M-Sn	^{nat}Sn	173.145 g	Rod	300 mm	10 mm
M-V	^{nat}V	7.188 g	Powder mix	100 mm	10 mm
M-Zn	^{nat}Zn	52.332 g	Rod	100 mm	10 mm
M-Zy4	^{nat}Zr	152.156 g	Rod	300 mm	10 mm
AlAu	^{nat}Au	0.6311 mg	Wires	100 mm	3 x 1.0 mm
C-Au-10	^{nat}Au	1.513 g	Rod	100 mm	1.0 mm
C-Au-16	^{nat}Au	3.854 g	Rod	100 mm	1.6 mm
C-Au-20	^{nat}Au	6.013 g	Rod	100 mm	2.0 mm

Samples design (size and type) has been optimized with regard to the neutronic effect of the isotopes studied [6]. Their reactivity worth in the core (proportional to their mass) is limited by the linearity range of the pilot rod (± 10 pcm). To account for a small cross-section, the sample mass has to be increased to obtain a suitable signal. Samples are usually made as rods of the natural element to achieve the highest material density (FIG 2, left). The diameter is limited by the aluminum clad inner diameter of 10 mm. In the case of nearly transparent materials (Sn, Zy4), the sample length has been increased to 300 mm (aluminum clad dimensions: 310 x 320 mm).
For the most reactive elements, the material of interest can be diluted either into a liquid acid matrix (H_2O + 5 % HNO_3) or into an alumina (Al_2O_3) powder matrix. Liquid samples are sealed into a watertight Zircaloy-4 welded clad, of 8.35 x 9.56 mm in diameter and 100 x 108 mm in height, and then inserted into an aluminum clad (FIG 2, right). It is a good way to decrease the spatial self-shielding effect and therefore increase the measurement sensitivity to the radiative capture cross-section [6].

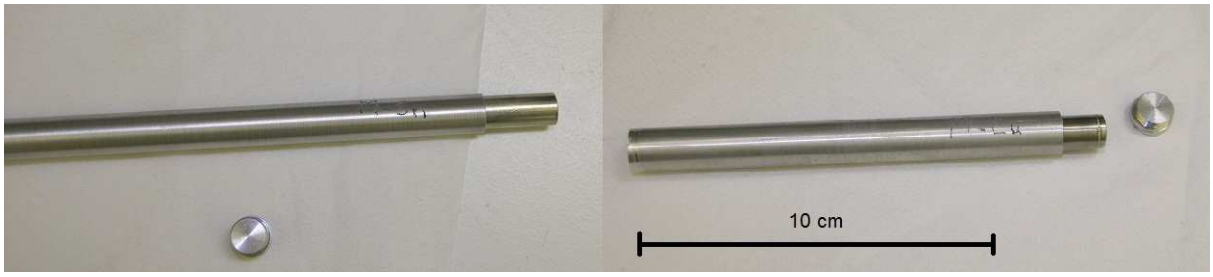

FIG 2: Tin rod sample (left) and liquid europium sample (right).

In reactor dosimetry measurements, ^{198}Au is generally considered as reference nuclide. To reduce uncertainties and to avoid as possible bias, results are presented as ratios of capture rates to the one of gold. Three of the reference samples are pure gold rods of 1.0 mm, 1.6 mm and 2.0 mm in diameter (respectively labelled C-Au-10, C-Au-16 and C-Au-20). A fourth one

is made of three aluminum-gold alloy wires of 1.0 mm in diameter, with 0.1 % gold in mass. The latter gives the gold reaction rate at infinite dilution.

The choice of the radio-isotopes to be measured is based on several conditions that must be fulfilled. In a simple way, the measured count rate *C* at energy *E* can be expressed as:

$$C(E) \propto \lambda \cdot \sigma_c \cdot I_\gamma(E) \cdot BR \quad (1)$$

where λ is the decay constant, σ_c the radiative capture cross-section, $I_\gamma(E)$ the emission intensity of the gamma ray at energy *E* and *BR* the branching ratio toward the measured nuclide. The product of those values must be high enough to get reliable and precise results. Also, the nuclide half-life should be at least 3 min to be measurable and the energy of the gamma rays must be within 100 keV – 1800 keV. Based on these criteria, the list of the studied radio-isotopes is given in Table II.

An additional set of small detectors was used to measure capture cross section cadmium ratios. Silver, gold, indium and cesium were studied. Their characteristics are given in the Table III. Except for cesium, which is a liquid sample, these detectors are small disks (< 0.5 mm height) of pure natural material.

TAB II: Measured radio-isotopes by neutron activation experiments.

Sample	Isotope	Radio-isotope	Half-life*	Number of gamma-rays
M-Eu	^{151}Eu	^{152}Eu	13.5 y	10
		^{152m}Eu	9.3 h	1
	^{153}Eu	^{154}Eu	8.6 y	3
M-In-2	^{113}In	^{114m}In	49.5 d	2
	^{115}In	^{116m}In	54.3 min	5
M-Ag-2	^{109}Ag	^{110m}Ag	249.8 d	3
M-Cs-2	^{133}Cs	^{134m}Cs	2.9 h	1
		^{134}Cs	2.1 y	5
M-Mo	^{98}Mo	^{99}Mo	2.7 d	4
	^{100}Mo	^{101}Mo	14.6 min	2
M-Sn	^{112}Sn	^{113}Sn	115.1 d	1
	^{116}Sn	^{117m}Sn	13.6 d	1
	^{122}Sn	^{123m}Sn	40.1 min	1
M-V	^{51}V	^{52}V	3.7 min	1
M-Zn	^{68}Zn	^{69m}Zn	13.8 h	1
	^{64}Zn	^{65}Zn	224.0 d	1
M-Zy4	^{94}Zr	^{95}Zr	64.0 d	2
	^{96}Zr	^{97}Zr	16.7 h	2
AlAu C-Au-10 C-Au-16 C-Au-20	^{197}Au	^{198}Au	2.7 d	1

* min = minute, h = hour, d = day, y = year

TAB III: Cadmium ratio detectors characteristics.

Detector	Element	Type	Height	Diameter	Isotope	Radio-isotope
Gold	^{nat}Au	Disk	50 µm	8 mm	^{197}Au	^{198}Au
Indium	^{nat}In	Disk	250 µm	8 mm	^{115}In	^{116m}In
Silver	^{nat}Ag	Disk	100 µm	8 mm	^{109}Ag	^{110m}Ag
Cesium	^{nat}Cs	Solution	Zy4 clad: 30.6 x 38.6 mm	Zy4 clad: 8.35 x 9.56 mm	^{133}Cs	^{134m}Cs

2.3 Gamma spectrometry bench

After a sample has been irradiated, gamma emission spectrum is measured by gamma spectrometry. The detector is a high-purity germanium (HPGe) planar crystal of 40 cm^3, with a resolution about 1 keV at low energies. It has been calibrated using standard gamma sources on the 50 - 1850 keV energy range.
Samples are held at a distance of 18.5 cm from the detector (19 cm from the germanium crystal) by a holder that rotates the sample about its axis to account for any radial heterogeneity in the capture rate (FIG 3). The distance has been chosen to optimize against coincidence summing and to increase count rate. The detector is shielded with a 5-cm thick tungsten block. The width of the lead + tungsten collimator has been determined so that the measured activity is independent on the sample length (10 or 30 cm). This way, the measured count rate is directly linked to a reaction rate per volume unit of the central part of the sample.

FIG 3: Picture of the gamma spectrometry bench.

The absolute efficiency of the detector was measured with standard gamma sources (^{241}Am, ^{109}Cd, ^{57}Co, ^{139}Ce, ^{51}Cr, ^{85}Sr, ^{137}Cs, ^{54}M, ^{88}Y, ^{65}Zn and ^{60}Co) acting as point sources. Those measurements were carried out at a source-detector distance of 24.5 cm (25 cm from the Ge crystal). The resulting calibration curve gives the relation between the point source total activity and its measured count rate in the detector for a gamma peak at energy *E*. This experimental curve is fitted using an APOLOG model [10]:

$$\log\left(R^P(E)\right) = \sum_{i=0}^{N} a_i \left(\log(E)\right)^i \qquad (2)$$

with $R^P(E)$ being the detector efficiency at energy *E*. In this study, the polynomial order was set to 6 ($N = 5$). The resulting calibration curve and its residuals are shown FIG 4.

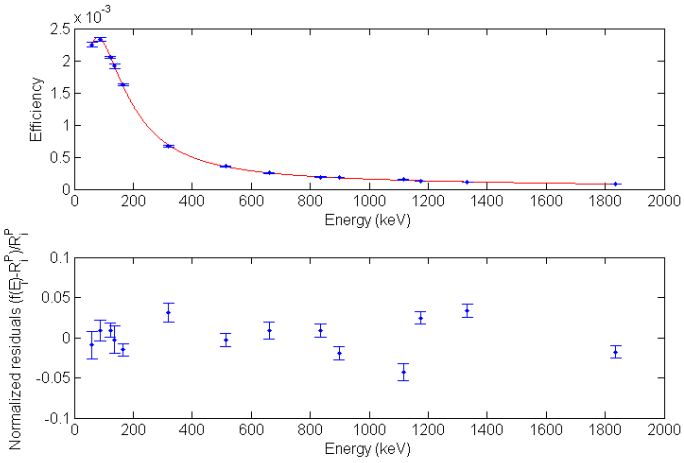

FIG 4: Experimental calibration curve (top) and normalized residuals (bottom).

To adjust the calibration curve at the sample measurement distance of 18.5 cm, a correction factor has been calculated using an MCNP5 [8] modelling of the gamma spectrometry bench (FIG 5). This correction factor loosely depends of the energy (1 % change between low and high energies), and its uncertainty is negligible.
To account for samples geometry an efficiency transfer factor is needed that corrects for the self-attenuation of the gamma rays inside the sample, and inside the surroundings materials (mainly the collimator). This factor is given by:

$$T(E) = \frac{\eta_v(E)}{\eta_0(E)} \quad (3)$$

where $\eta_v(E)$ the deposited energy in the detector for the sample, and $\eta_0(E)$ the deposited energy in the detector for a point source. To calculate η_v, the capture rate distribution in the sample volume is fed to the MCNP bench simulation.

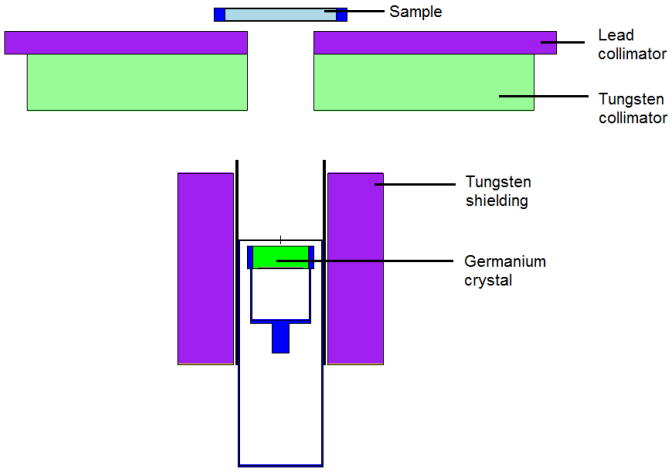

FIG 5: MCNP model of the gamma spectrometry bench with a 10-cm long sample.

3. Experimental results and uncertainty analysis

3.1 Irradiation setup

Samples are irradiated inside the oscillating device. When the reactor power is stable, the oscillating device is quickly inserted in the irradiation channel (sample at the mid-core plane). The power is maintained constant thanks to the automatic piloting system. At the end of the irradiation, the control rods are dropped to shut down immediately the reactor power.
For the cadmium ratios measurements, dosimeters are inserted inside a 20-mm long and 9-mm diameter aluminum container, and then put inside an aluminum clad. For the second irradiation, the container is wrapped with a 1-mm cadmium foil.
The reactor power was set to 80 W for all irradiations, except for the gold dosimeter (10 W). The duration was adjusted depending on the sample. All irradiations are monitored with a miniature fission chamber (MFC) [9]. The MFC is located outside the driver zone in the graphite reflector. All measurements are normalized to its count rate (related uncertainty is negligible).
After a suitable cooling time – from a few ten of seconds to an hour – samples are measured on the spectrometry bench. The acquisition sequence (duration and number of measurements) depends on the half-life of the activation product to be measured.

3.2 Data processing and uncertainties

The integral capture rate of a sample is given by the following relationship:

$$\Sigma_c \Phi = \frac{N_{sat}(E,d)}{I_\gamma(E) R^P(E,d) T(E,d,d_0)} \quad (4)$$

where $N_{sat}(E,d)$ is the saturation count rate of the gamma peak at energy E and distance d, $I_\gamma(E)$ is the emission intensity of the gamma ray, $R^P(E,d)$ is the detector efficiency at energy E and distance d, and $T(E,d,d_0)$ the calculated efficiency transfer, including the distance correction. From the measurement, saturation count rate is given by:

$$N_{sat}(E,d) = \frac{N(E,d)}{t_m} C_\theta C_{dec} \quad (5)$$

where $N(E,d)$ is the peak net area at energy E and distance d, t_m is the active measurement time, C_θ the dead-time correction factor and C_{dec} the decay correction factor. This factor corrects the radioactive decay of the nuclide (with λ its decay constant) during irradiation, cooling and real measurement times (respectively t_i, t_o, and t_r):

$$C_{dec} = \frac{\lambda t_m}{e^{-\lambda t_o}(1-e^{-\lambda t_i})(1-e^{-\lambda t_r})} \quad (6)$$

If a sample is measured after a second irradiation, a residual activity coming from the first irradiation has to be taken into account:

$$N_{sat}(E,d) = \left(\frac{N(E,d)}{t_m} C_\theta - \frac{N_{res}(E,d)}{t_{m,res}} e^{-\lambda \delta t} C_{\theta,res}\right) C_{dec} \quad (7)$$

where the subscript *res* refers to the residual measurement, done before the second irradiation. δt is the time between residual and post-irradiation measurements. The peak net area is obtained by a Gaussian fit of the gamma peak.

Each measurement is normalized to each one of the gold reference sample:

$$\frac{\Sigma_c \Phi|_{sample}}{\Sigma_c \Phi|_{gold}} = \frac{N_{sat}(E,d)|_{sample}}{N_{sat}(E,d)|_{gold}} \frac{I_\gamma(E)|_{gold}}{I_\gamma(E)|_{sample}} \frac{T(E,d,d_0)|_{gold}}{T(E,d,d_0)|_{sample}} \frac{R^P(E,d)|_{gold}}{R^P(E,d)|_{sample}} \frac{C_{mon}|_{gold}}{C_{mon}|_{sample}} \quad (8)$$

where C_{mon} is the monitor count rate.

Detector efficiencies for both samples are correlated trough the calibration curve. The ratio of the efficiencies and its uncertainties are directly computed to take into account this correlation. This uncertainty ranges from less than 0.1% (for gamma peaks very close in energy to the 411.8 keV gold gamma ray) to 0.9%. All the other terms are considered uncorrelated. Uncertainty of the efficiency transfer comes from the numerical convergence of the Monte Carlo calculation; it varies between 0.1% and 0.5%. The uncertainty on the saturation activity is linked to the count rate statistics and the decay constant uncertainty and lies between 0.1 % and 3 %.

Cadmium ratios are relative measurements as well. Most of the terms required for absolute capture rate measurements are cancelled. The formula is the following:

$$R_{Cd} = \frac{N_{sat}}{C_{mon} m_{det}} \frac{C_{mon,Cd} m_{det,Cd}}{N_{sat,Cd}} \quad (9)$$

where m_{det} is the mass of the detector. The subscript *Cd* refers to the irradiation with the cadmium shielding.

All nuclear data (half-life and gamma-ray emission intensities) used in the analysis come from LNHB [11], except for ^{123m}Sn [12] and ^{97}Zr [13].

3.3 Activation measurements results

For some radio-isotopes, it was possible to compare results from different gamma rays. Each time, a good agreement was obtained, and results were consistent with regard to uncertainties. Results are given on FIG 6 to FIG 8. For example, the 10 studied gamma rays of ^{152}Eu are in fairly good agreement, with uncertainties lying between 1 % and 2 % (FIG 6, left).

Eventually, all gamma-ray results are combined, to obtain a global value for the isotope capture rate. The overall experimental results of the activation measurements are given in Table IV. Measurements for In, Cs and Ag liquid samples were made several months after the other samples. At this time, only two of the gold reference samples were also irradiated to normalize the measurements: C-Au-10 and C-Au-16.

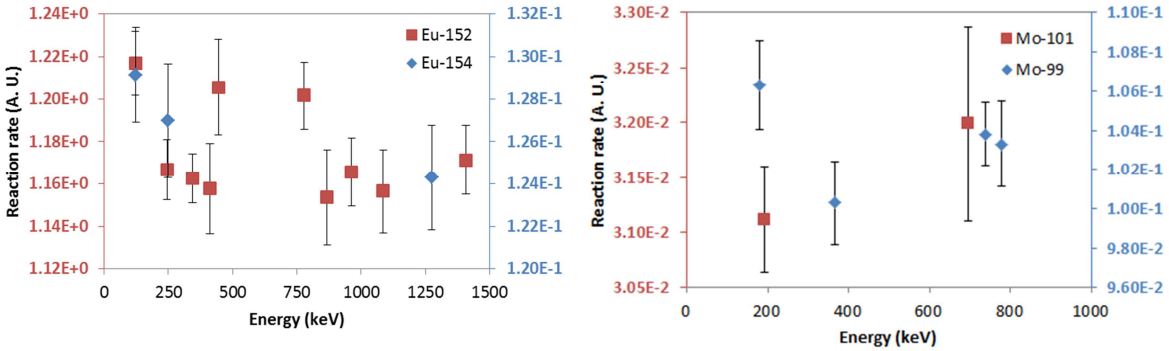

FIG 6: Left: results for ^{152}Eu (left-hand axis) and ^{154}Eu (right-hand axis). Right: results for ^{101}Mo (left-hand axis) and ^{99}Mo (right-hand axis) (1σ).

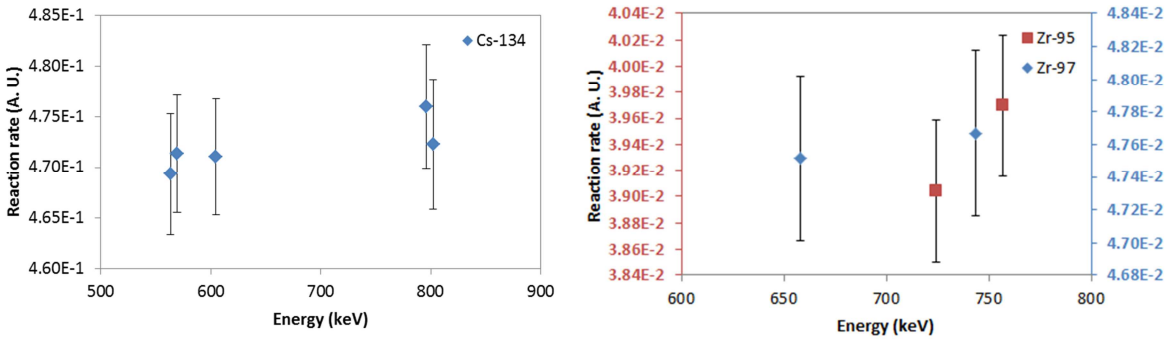

FIG 7: Left: results for ^{134}Cs. Right: results for ^{95}Zr (left-hand axis) and ^{97}Zr (right-hand axis) (1σ).

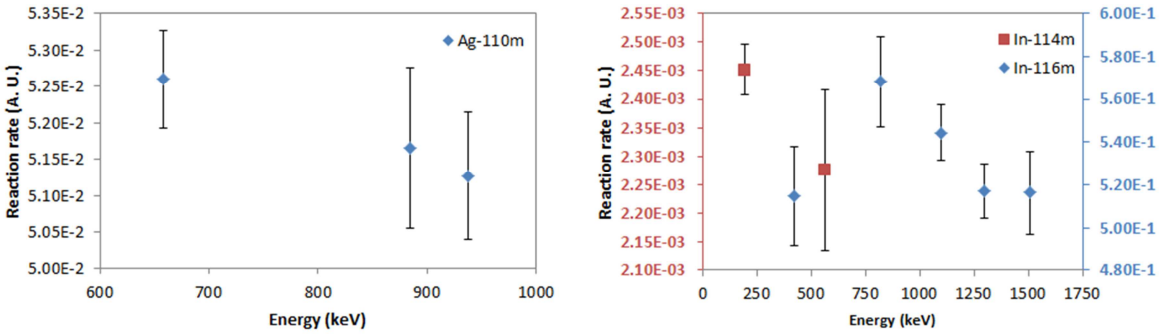

FIG 8: Left: results for ^{110m}Ag. Right: results for ^{114m}In (left-hand axis) and ^{116m}In (right-hand axis) (1σ).

TAB IV: Experimental results of activation measurements (1σ).

Measured isotope	X/AlAu		X/C-Au-10		X/C-Au-16		X/C-Au-20	
	Ratio	σ (%)	Ratio	σ (%)	Ratio	σ (%)	Ratio	σ (%)
^{152}Eu	7.03E+2	0.6%	1.18E+0	0.5%	5.43E-1	0.5%	3.87E-1	0.6%
^{152m}Eu	3.72E+2	2.2%	6.14E-1	2.0%	2.83E-1	2.0%	2.02E-1	2.2%
^{154}Eu	7.64E+1	1.3%	1.27E-1	1.1%	5.86E-2	1.1%	4.15E-2	1.3%
^{101}Mo	1.87E+1	1.6%	3.13E-2	1.4%	1.44E-2	1.4%	1.02E-2	1.5%
^{99}Mo	6.21E+1	1.1%	1.03E-1	1.0%	4.77E-2	1.0%	3.37E-2	1.1%
^{113}Sn	5.15E+1	1.4%	8.63E-2	1.3%	3.99E-2	1.3%	2.80E-2	1.3%
^{117m}Sn	4.47E+1	1.5%	7.49E-2	1.5%	3.46E-2	1.5%	2.43E-2	1.5%
^{123m}Sn	1.66E+1	1.5%	2.77E-2	1.5%	1.28E-2	1.5%	8.98E-3	1.5%
^{52}V	5.14E+2	1.4%	8.56E-1	1.2%	3.95E-1	1.2%	2.79E-1	1.4%
^{65}Zn	2.66E+2	2.0%	4.42E-1	1.3%	2.04E-1	1.3%	1.44E-1	2.0%
^{69m}Zn	1.05E+1	1.3%	1.76E-2	0.9%	8.09E-3	0.9%	5.71E-3	1.2%
^{95}Zr	2.38E+1	1.7%	3.94E-2	1.0%	1.81E-2	1.0%	1.29E-2	1.7%
^{97}Zr	2.83E+1	1.0%	4.76E-2	0.8%	2.20E-2	0.8%	1.54E-2	1.0%
^{114m}In	-	-	2.44E-3	1.8%	1.12E-3	1.8%	-	-
^{116m}In	-	-	5.31E-1	1.4%	2.43E-1	1.4%	-	-
^{134}Cs	-	-	4.72E-1	0.6%	2.16E-1	0.6%	-	-
^{134m}Cs	-	-	4.37E-2	3.5%	2.00E-2	3.5%	-	-
^{110m}Ag	-	-	5.20E-2	0.9%	2.38E-2	0.9%	-	-

To compare results for the different reference samples, the self-shielding factor of the gold samples were obtained with a Monte Carlo calculation (Table V). The ratios of the macroscopic cross sections to gold at infinite dilution are given for each capturing nuclide in Table VI. When necessary, those results are calculated using the branching ratio of the measured nuclide. Branching ratios values come from [14]. A constant 0.5 % uncertainty has been added to take into account for potential modeling and calculation uncertainties.

TAB V: Gold samples self-shielding factors.

Sample	Reaction rate (s^{-1})	Self-shielding factor
AlAu	2.3104E-08	1.0
C-Au-10	1.3762E-05	595.7
C-Au-16	3.0119E-05	1303.6
C-Au-20	4.3213E-05	1870.4

TAB VI: Ratios of the macroscopic capture cross section to gold at infinite dilution (1σ).

Isotope	Macroscopic cross sections	
	Ratio	σ (%)
^{151}Eu	1.08E+03	1.0%
^{153}Eu	7.76E+01	1.3%
^{100}Mo	6.22E+01	1.6%
^{98}Mo	1.88E+01	1.2%
^{112}Sn	7.13E+01	1.4%
^{116}Sn	1.10E+03	1.6%
^{122}Sn	1.68E+01	1.6%
^{51}V	5.14E+02	1.4%
^{64}Zn	5.51E+02	1.8%
^{68}Zn	5.55E+01	1.2%
^{94}Zr	2.36E+01	1.5%
^{96}Zr	2.85E+01	1.1%
^{113}In	2.50E+00	1.9%
^{115}In	8.90E+02	1.5%
^{133}Cs	3.07E+02	0.8%
^{109}Ag	6.74E+02	1.0%

3.4 Cadmium ratio measurements results

For the indium dosimeter, 5 gamma rays were measured. Results are consistent within their statistical uncertainty range (Table VIII).

TAB VIII: Experimental ^{116m}In cadmium ratios (1σ).

Energy (keV)	Cadmium ratio	Statistical uncertainty
416.86	2.822	0.13%
818.7	2.833	0.25%
1097.3	2.835	0.15%
1293.54	2.829	0.14%
1507.4	2.833	0.34%

Because it has the highest radiative capture cross section in the thermal and epithermal domain, the ^{115}In has the highest cadmium ratio (Table IX and FIG 9). The final total uncertainty takes into account contributions linked to the gamma measurement process (positioning and measurement reproducibility).

TAB IX: Cadmium ratio measurements results (1σ).

Dosimeter	Isotope	Cadmium ratio	Total uncertainty
Au	^{197}Au	1.93	0.7%
Ag	^{109}Ag	1.80	1.1%
In	^{115}In	2.83	0.7%
Cs	^{133}Cs	1.89	0.7%

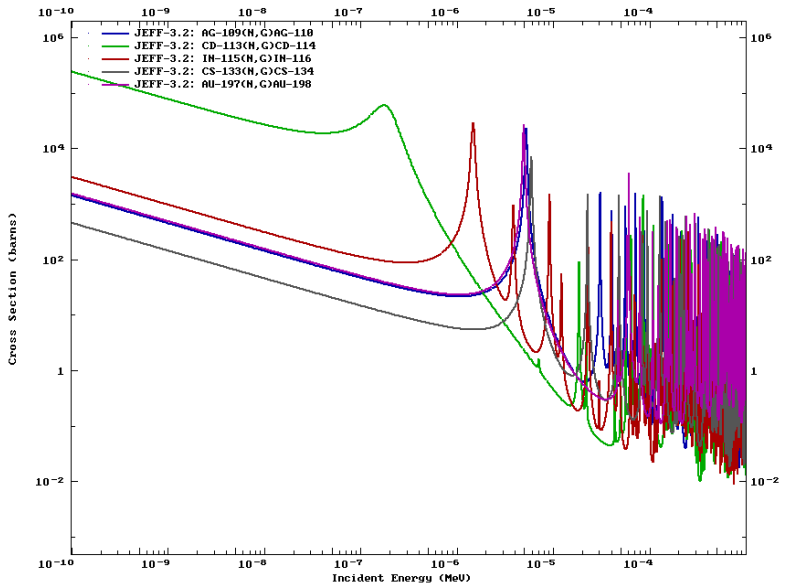

FIG 9: Radiative capture cross section of ^{109}Ag, ^{197}Au, ^{115}In, ^{133}Cs and ^{113}Cd.

4. Conclusion

Oscillation and activation measurements carried out in the MINERVE reactor are designed to obtain reliable and precise information on the integral cross section of isotopes or materials, in a well characterized neutron field. The MAESTRO program was devoted to the improvement of neutron cross sections of elements such as neutron absorbers, detection materials and reactor structure materials used in Gen-II and –III PWRs. The neutron spectrum achieved in the center of the MINERVE core is representative of a typical PWR spectrum loaded with UO_2 fuel pins.

During the activation phase of the program, 9 samples of natural elements were studied, corresponding to the measurement of 16 radio-isotopes by gamma spectrometry. Although measurements were carried out during a large period of time, results show good consistency against the various reference samples.
The re-assessment of the radiative capture cross section for the mentioned isotopes should be completed with oscillation measurements also performed during this experimental program.
Future work on the data collected during this experimental program could include the re-assessment of the half-life of a few nuclides, or of the gamma ray emission intensity (In, Cs, Ag, Eu), by combining neutron activation and oscillation measurements. Integral information about several branching ratios in a typical PWR spectrum could also be obtained through those measurements.

5. Acknowledgments

This work was financed by CEA, EdF and AREVA-NP.
The authors would like to thank the operators team of the MINERVE facility.

6. References

[1] A. Gruel *et al.*, Interpretation of Fission Product Oscillations in the MINERVE Reactor, from Thermal to Epithermal Spectra, Nucl. Sci. Eng., vol. 169, no. 3, pp. 229–244.
[2] J.-P. Hudelot *et al.*, OCEAN, an ambitious experimental program for the qualification of integral capture cross sections of neutron absorbers, PHYSOR 2006 International Conference.
[3] D. Bernard *et al.*, Validation of actinides nuclear cross section using pile-oscillation experiments performed at MINERVE facility, J Korean Phys. Soc., vol. 59, no. 2, pp.1119-1122.
[4] P. Fougeras, A. Chabre, C. Mergui, The place of EOLE, MINERVE and MASURCA facilities in the R&D activities of the CEA, Proc. Int. Conf. IGORR 2005, Gaitherburg, USA, 2005.
[5] M. Antony *et al.*, Oscillation experiments techniques in CEA MINERVE experimental reactor, in 2009 1st International Conference on Advancements in Nuclear Instrumentation, Measurement Methods and their Applications (ANIMMA), 2009.
[6] P. Leconte *et al.*, MAESTRO: An ambitious experimental programme for the improvement of nuclear data of structural, detection, moderating and absorbing materials - First results for natV, 55Mn, 59Co and 103Rh, in 2013 3rd International Conference on Advancements in Nuclear Instrumentation, Measurement Methods and their Applications (ANIMMA), 2013.
[7] W. K. Foell, A. N. Society, and U. S. A. E. Commission, Small-sample reactivity measurements in nuclear reactors. 1972.
[8] X-5 Monte Carlo Team, MCNP — A General Monte Carlo N-Particle Transport Code, Version 5, LA-UR-03-1987, 2005.
[9] B. Geslot *et al.*, Development and manufacturing of special fission chambers for in-core measurement requirements in nuclear reactors, in 2009 1st International Conference on Advancements in Nuclear Instrumentation, Measurement Methods and their Applications (ANIMMA), 2009.
[10] G.L. Molnár, Zs. Révay, T. Belgya, Wide energy range efficiency calibration method for Ge detectors, Nuclear Instruments and Methods in Physics Research Section A: Accelerators, Spectrometers, Detectors and Associated Equipment, Volume 489, Issues 1–3, 21 August 2002, Pages 140-159.

[11] LNHB, PTB/E. Schönfeld, R. Dersch (1998), http://laraweb.free.fr/
[12] A. Santamarina *et al.*, The JEFF-3.1.1 Nuclear Data Library, JEFF Report 22, OECD 2009, NEA N^{o} 6807
[13] N. Nica, Nuclear Data Sheets for A = 97, Nuclear Data Sheets 110, 2010, pp. 525–716.
[14] J.-C. Sublet *et al.,* The European Activation File: EAF-2010 neutron-induced cross section library, CCFE-R (10) 05.